ACS OMEGA

Open Access

http://pubs.acs.org/journal/acsodf

Article

Improving Fine Particle Removal Using a Single-Channel Slit Bubbling Device in Wet Flue Gas Desulfurization System

Can Fang, Yi Xiao, Wencong Qiu, Haoyu Zhang, Tianyu Zhao, Renjie Zou,* Guangqian Luo,* and Hong Yao

Cite This: *ACS Omega* 2024, 9, 9321−9330

Read Online

ACCESS | Metrics & More | Article Recommendations | Supporting Information

ABSTRACT: To improve the cleanliness of coal-fired power plants' particulate matter emissions, a novel device (single-channel slit bubbling particle removal device (SCSB-PRD)) is proposed to improve the wet flue gas desulfurization system's (WFGDs) collaborative particle removal effect. Actual coal-fired flue gas was used to test the particle removal performance. The results showed that the flue gas temperature had no obvious effect on the scrubbing effect of the SCSB-PRD. The scrubbing space, scrubbing liquid volume, and flue gas flow rate effectively changed the gas−liquid flow state, and the bubbling state was the key factor in particle removal. The jet-bubbling contact state was more conducive to removing particles than the foam bubbling state. The jet-bubbling state improved the removal efficiency of fine particles by approximately 30% compared to the foam bubbling state. The device operated in a single stage, and the removal performance of the particulate matter reached more than 60%. Even the submicron particles had a satisfactory removal performance of greater than 50%. The particulate matter concentration at the outlet of the WFGDs was reduced to less than 10 mg/m^3, which provides a feasible transformation path for ultraultra-low emissions of particulate matter from coal-fired power plants.

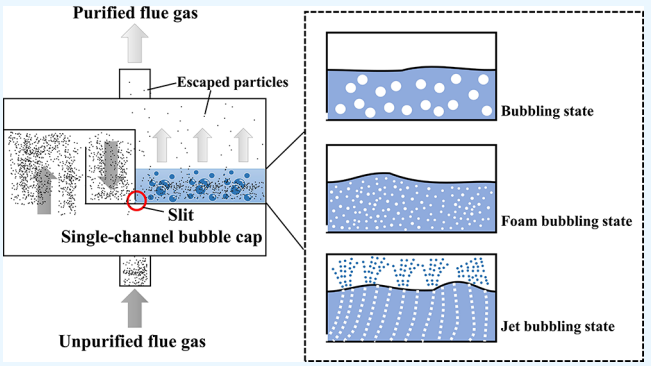

1. INTRODUCTION

Beginning in 1882, the demand for coal energy surged when the first coal-fired power plant was developed by Edison in New York City. Coal was burned to produce high-pressure steam that was passed into a turbine to generate electricity.[1] Coal continues to be the backbone source of our primary energy. In the World Energy Outlook 2021 publication, the share of coal in 2020 of the world's total energy supply reached 26.45%.[2] China accounted for over 50% of the global coal consumption in 2020 due to the country's energy structure and unfinished clean energy transition.[3]

China has released a series of policies to promote its energy consumption structure transition to clean energy.[4−6] However, energy consumption structure reform requires huge technological innovations and enormous financial support, and it will take a considerable amount of time to accomplish the transition. The State Grid Energy Research Institute prediction results showed that in 2035 and 2050, the share of China's coal-fired power generation will be 42.7 and 8.4%, respectively.[7]

Particulate matter (PM), which is a complex mixture of small particles found in coal combustion products, flows into the flue gas. An increased ambient PM concentration has been associated with increased respiratory diseases, lung cancer, and an increased incidence of stroke and heart attacks.[8−10] The Institute for Health Metrics and Evaluation stated that the estimated deaths in China attributed to ambient PM pollution exposure in 2019 were more than one million.[11]

In response to the enormous damage caused by PM, China has released a series of policies to guide domestic air PM concentration reductions.[12−14] In 2015, China issued the harshest ever coal-fired power plant pollution ultralow emission standard,[15] with a PM emission concentration of <10 mg/Nm^3. The national average $PM_{2.5}$ concentration in China declined from 72 μg/m^3 in 2013 to 33 μg/m^3 in 2020, and the PM_{10} concentration declined from 118 μg/m^3 in 2013 to 56 μg/m^3 in 2020, both displaying a decrease of more than 50%.[16] However, in the air quality guidelines released by the World Health Organization, the $PM_{2.5}$ air quality guideline level was set at 5 μg/m^3, and PM_{10} was set at 15 μg/m^3.[17] This means that more stringent restrictions are required to control PM pollution in China.

Received: October 28, 2023
Revised: December 12, 2023
Accepted: January 8, 2024
Published: February 14, 2024

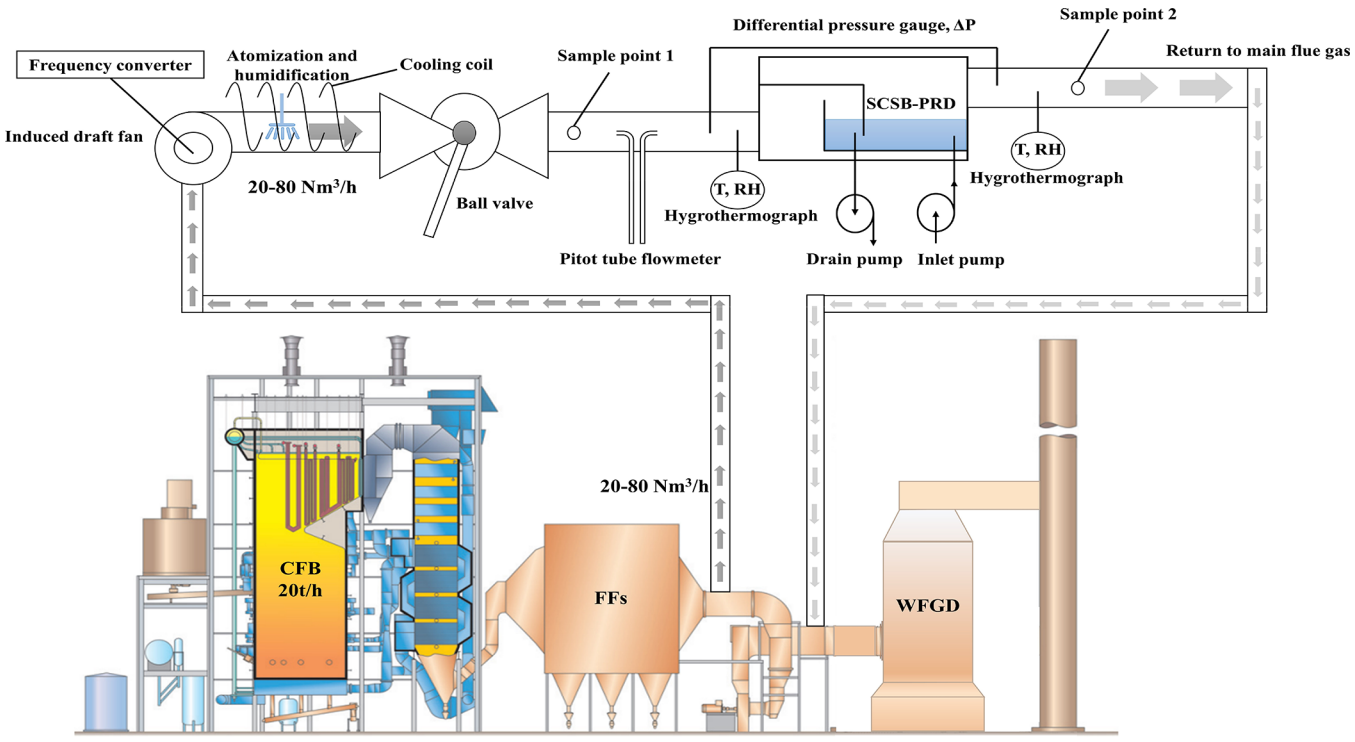

Figure 1. Schematic of the experimental pipelines, instruments, and devices.

In a coal-fired power plant, the primary PM emission control technologies include electrostatic precipitators or fabric filter (FF) dry PM removal technology, wet flue gas desulfurization (WFGD) system synergistic PM removal, and wet electrostatic precipitators (WESPs).[18] These are required for an ultraultra-low emission control technology route. Until 2030, the PM emission concentration from a coal-fired power plant will be less than 1 mg/Nm^3, achieving ultralow standards.[19]

In an explanation of the compilation of the Jiangsu Province Emission Standard of Air Pollutants for Thermal Power Plants, the PM removal efficiency of the WESPs installed in coal-fired power plants in Jiangsu Province was approximately 90%.[20] The Huadian Electric Power Research Institute[21] tested the PM emissions at the inlet and outlet of the WESPs in 26 ultralow emission units, and the results showed that the PM removal efficiency of the WESPs was approximately 90%. Hence, to achieve ultraultra-low PM emission standards, it is necessary to ensure that the concentration of particulates at the outlet of a WFGD system is below 10 mg/Nm^3. However, according to the Huadian Electric Power Research Institute test results, in an explanation for the compilation of the Jiangsu Province "Emission Standard of Air Pollutants for Thermal Power Plants"[21,22] and statistics from publications, the results showed that the concentration of particulates at the exit of an existing WFGD device was 15−20 mg/m^3. Therefore, to achieve ultraultra-low PM emission standards, it is necessary to strengthen the PM removal efficiency in WFGD systems, and the PM concentration in a WFGD outlet must be less than 10 mg/m^3.

The mechanism of particle removal in a WFGD system occurs when the flue gas and spray droplets are in reverse flow, and the PM that is entrained by the flue gas is trapped by the droplet due to its contact with the droplet surface.[23,24] The PM flow is affected by the particle inertial force, Brownian motion, the thermophoretic force, the diffusional force, the drag force, and interception.[25−27] Rafidi et al.[28] simulated PM removal with a WFGD system using the computational fluid dynamics method. The results showed that an unsatisfactory PM removal performance occurred when the particle diameter was within 0.1−2 μm. Huang et al.[29] used the Monte Carlo method to simulate PM removal by droplets in a WFGD system. They found that the PM removal efficiency decreased with an increase in the droplet size. The Brownian motion mechanism dominates the PM removal when the particulate diameter is less than 0.01 μm. The inertia mechanism dominates the PM removal process when the particle size is greater than 2 μm. To achieve a high PM removal performance, a fine mist droplet removal technology was invented. Liang et al.[30] designed three spray nozzles for PM removal, and the droplet diameter was less than 1 mm to achieve a high PM removal. However, the existing WFGD devices have a weak PM removal efficiency due to limitation of the droplet size. When the droplet size is less than 2 mm, the droplets will be entrained by the flue gas and escape, forming the "gypsum rain" phenomenon. The escaped droplets are a primary source of PM.[31−33] Therefore, reducing the droplet size to strengthen PM removal is not suitable for WFGD devices.

Under this circumstance, researchers investigated the particle capture performance in another gas−liquid flow state, bubble flow. Particles are trapped by the bubble while particles move to the gas−liquid interface due to the drag force, the inertial force, the Brownian force, and the thermophoresis force.[34−37] The bubble flow is inconsistent with the droplet flow, where there are no size limitations for the bubbles.

In industry, the most commonly used bubbling devices include a bubble column, a sieve tray tower, a bubblecap tower, a fixed valve tray column, and a vortex scrubber.[38−42] The common feature of these devices is that the gas that flows through the bubbling structure (slits and holes) interacts with

https://doi.org/10.1021/acsomega.3c08250
ACS Omega 2024, 9, 9321−9330

the liquid and generates bubbles. Terasaka et al.[43] investigated the effect of the bubble morphology using a slits and holes structure. The results showed that the structure of the hole tended to generate larger bubbles that had smaller specific surface areas, while the bubbles generated by the slit were smaller and more uniformly distributed than those generated by the hole structure. The slit structure was more conducive to PM purification.[44,45]

To achieve the PM ultraultra-low emission standard, new technology desperately needs to be developed. In this study, a slit bubbling structure is developed and designed to purify the PM in a coal-fired flue gas WFGDs. In order to investigate the performance and mechanism of the device on the actual flue gas particulate removal, the actual coal-fired flue gas is used to carry out experimental studies on particulate removal to obtain the optimization of the parameters of the bubbling device and the removal mechanism. The structure of this article is as follows. Section 1 is the introduction. Section 2 presents the experimental details, including the experimental device, and the measurement technique. Section 3 presents an analysis of the experimental results including a reliability verification of the experimental results and the influence of the experimental parameters on the particle capture performance. The conclusion and discussion are provided in Section 4.

2. EXPERIMENT

2.1. Experimental Setup. The flue gas was provided by a circulating fluidized bed boiler (CFB), as shown in Figure 1. The flue gas from the CFB passed through the FFs and WFGDs. The flue gas with approximately 50,000 N m^3/h was provided by CFB coal combustion. Due to the relatively cleaner anthracite coal source and relaxed emission standard for industrial boilers, the NOx concentration met the emission standards without direct purification. While the flue gas carried particles that passed through the FFs, the coarse particles were removed and the flue gas entered the WFGDs for desulfurization. The flue gas was then purified and emitted into the atmosphere. A total of 20−80 N m^3/h of flue gas flowed out through an induced draft fan between the FFs and the WFGDs and then flowed into the particle removal device (PRD). The flue gas entered the primary flue pipeline after being purified by PRD. In the practical application of a power plant, the device can be installed inside the WFGD unit to improve the particle removal efficiency.

The induced draft fan, the experimental device, and the pipeline depicted in Figure 1, introduced particles and flue gas into the PRD through the pipeline. The induced draft fan (Y5-47, Taizhou Junlan Electromechanical Co. Ltd., China) included an atomizer (Dongguan Jieyuan Spray Equipment Co., Ltd., China), a frequency converter (EV-4300, Delta Electronics, Inc., Taiwan), a ball valve (Wenzhou Hegu Trading Co. Ltd., China), a pitot tube flowmeter (H8000B, Hangzhou Electronic Market Dingwang Electronic Firm, China), a differential pressure gauge (Pushida Sensing Technology Co., Ltd., China), a hygrothermograph (CJ 602, Yueqing Beita Electric Co. Ltd., China), and an inlet pump and drain pump (60W electric micro diaphragm pump, Ningbo Leicheng Pump Co., Ltd., China). The flue gas flow rate could be adjusted from 20 to 80 N m^3/h using a frequency converter and ball valve. The flue gas temperature and humidity could be adjusted using a cooling coil and an atomizer spray controlled by a peristaltic pump. The flow rate was monitored using a pitot tube flowmeter. A hygrothermograph and differential pressure gauge were installed in the single-channel slit bubbling particle removal device (SCSB-PRD) flue gas inlet and outlet to monitor the flue gas temperature, humidity, and system pressure drop. The inlet pump and drain pump were responsible for the SCSB-PRD scrubbing water level control. A pitot tube flowmeter was used for flue gas flow flux monitoring. Sample points were located in the SCSB-PRD front and rear for the equi-velocity sampling of PM. The above devices were established to explore the particle removal performance of the SCSB-PRD.

Figure 2 depicts the geometric details of the SCSB-PRD. The flue gas entrained with particles entered the particle

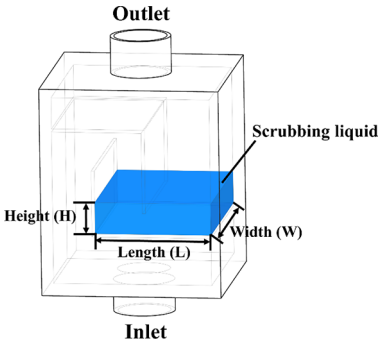

Figure 2. Geometric diagram of the SCSB-PRD.

scrubbing device through a 20 mm high slit, arousing a large number of bubbles. The scrubbing device consisted of a scrubbing pool, and the primary characteristic parameters consisted of the initial scrubbing liquid volume, that is, the length (L), width (W), and height (H).

In the experiment, tap water at 25 °C was used as the scrubbing liquid, the flue gas temperature in the FF outlet was approximately 120 °C, the relative humidity was approximately 10%, the SO_2 concentration was approximately 200 mg/m^3, and the PM concentration was approximately 25 mg/m^3.

For the newly developed PRD, SCSB-PRD was installed in the outlet of the WFGD, below the mist eliminators. The designed system used an additional circulation system through water scrubbing, and the SCSB-PRD was a component of the bubble cap tray scrubbing device. The detailed structure and installed position can be seen in Figure 3. However, the slit size of the SCSB-PRD was selected to be the classic bubble cap tray slit size, which was not considered in this work.

2.2. Measurement Technique. The Andersen cascade impactor was selected for PM concentration monitoring in this study, because of its high reliability and accuracy. A schematic of the Andersen cascade impactor (TE-20-800, TISCH Environmental, Inc., OH, USA) sampling device is shown in Figure S1a. It consisted of a PM sample gun, an Andersen cascade impactor, a flow control valve, a float flowmeter, and a vacuum pump (maximum flow: 28.3 L/min). Anderson cascade impactors have eight stages of particle size classification (0.43−9 μm), and particles that are larger than 10 μm in diameter are cut by the preseparator. The Andersen cascade impactor was developed from particles classified by the human respiratory tract based on particle aerodynamics.[46,47] PM deposition varied with the particle size, shape, density, and physicochemical properties of the particles that constitute the aerodynamic dimensions (Figure S1b).

The Andersen cascade impactor method for particulate matter sampling is widely used in the literature to classify

https://doi.org/10.1021/acsomega.3c08250
ACS Omega 2024, 9, 9321−9330

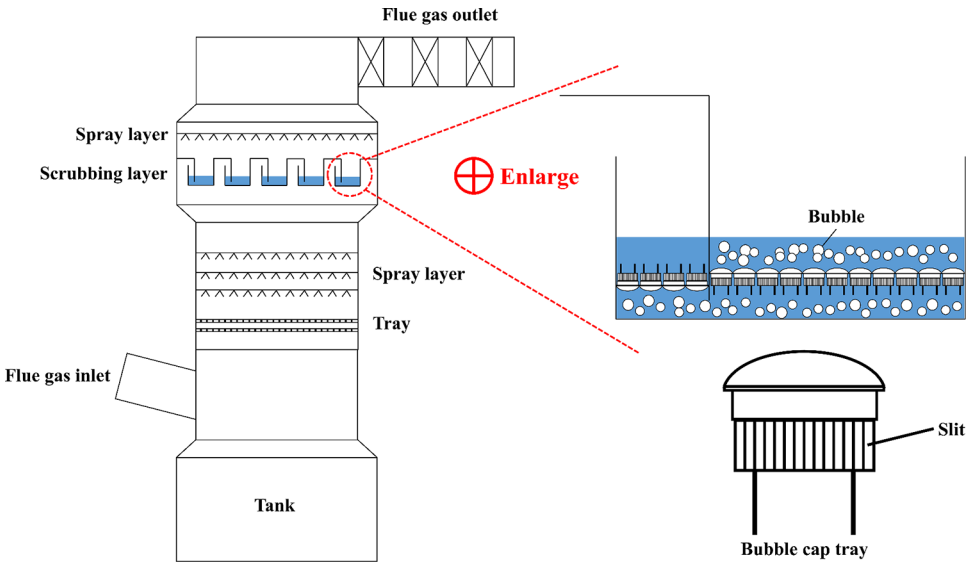

Figure 3. Detailed structure and installed position of the bubble cap tray scrubbing layer.

particulate matter sampling, and its accuracy has been extensively verified in the literature as a very effective and accurate method of classifying particulate matter for sampling.[46,47]

The Anderson cascade impactors consist of a preseparator size selective inlet (>10 μm), seven orifice stages, nine substrate collection plates, one filter stage, and base plate. When sampled flue gas flow through the impactor, the multiple orifice jets on each stage direct particles toward an impaction surface directly below each orifice. The impaction surface is referred to an 81 mm diameter quartz microfiber filter. The aerodynamic characteristic of a particle is determined by impact behavior. All particles with insufficient inertia to break out of the sample flow streamlines to be impacted on the first collection plate will follow the flue gas through the exhaust vents and into the following stage. It will then either be impacted on the next collection plate or passed to the succeeding impactor stage. The jet velocity of each succeeding orifice stage increases until the back-up filter collects the submicron particles by filtration.

3. RESULTS AND DISCUSSION

3.1. Experimental Reliability Verification. *3.1.1. Particulate Matter Deposition Loss in the SCSB-PRD.* Given the deposition of PM in the pipeline and the SCSB-PRD, the device itself has a certain ability to remove PM without the addition of a scrubbing liquid. Hence, a PM deposition loss experiment was conducted in this study. As shown in Figure 4, the naming rule was X-Concentration, where X represents the sample points (Points 1 and 2). The results showed that the PM loss rate was extremely low (<10%) and could be ignored. The particle size distribution before and after the SCSB-PRD showed good consistency, which indicated that the reliable sampling process and the device itself had little effect on the particle removal performance.

3.1.2. Experimental Repeatable Verification Using the Scrubbing Process. Because actual coal-fired flue gas was extracted and used as the PM source in this particle removal experiment, this resulted in the flue gas temperature, PM concentration, and particle size distribution having certain fluctuations attributed to the complexity of the combustion

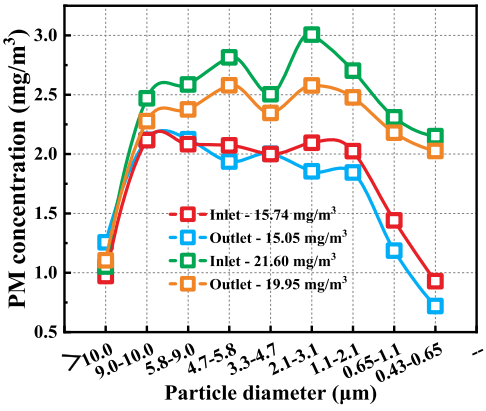

Figure 4. Plot showing the particle loss characteristics in the SCSB-PRD.

conditions of industrial CFB. Different particle concentrations and particle sizes have different capture efficiencies because particles with different particle sizes have different motions and capture mechanisms.[35] Hence, it was impossible to replicate each set of experiments. The experiments were repeated at similar concentrations and consistent scrubbing experimental conditions. The particle concentration at the SCSB-PRD inlet was approximately 25 mg/Nm^3, and the particle removal efficiency was approximately 68% (Figure S2). While the naming rule was X-Y-Concentration, where X represents the experimental serial number (e.g., first, second, and third), and Y represents the sample points (Points 1 and 2). The result indicated the reliability and stability of the device's particle removal results.

3.2. Effect of the Flue Gas Temperature on the Particle Removal Performance. Figure 5 shows the PM removal performance of graded particle sizes at different flue gas temperatures (70−90 °C). The flue gas relative humidity was constrained to 10% at 100 °C. During the scrubbing process, the bubbling space of the SCSB-PRD remained at L37W150H40 (L = 37 mm and W = 150 mm), the initial liquid height (H) remained at 40 mm; we adjusted the washing liquid volume to remain essentially unchanged by adjusting the inlet and drain pump, and the flow of the flue gas remained

https://doi.org/10.1021/acsomega.3c08250
ACS Omega 2024, 9, 9321−9330

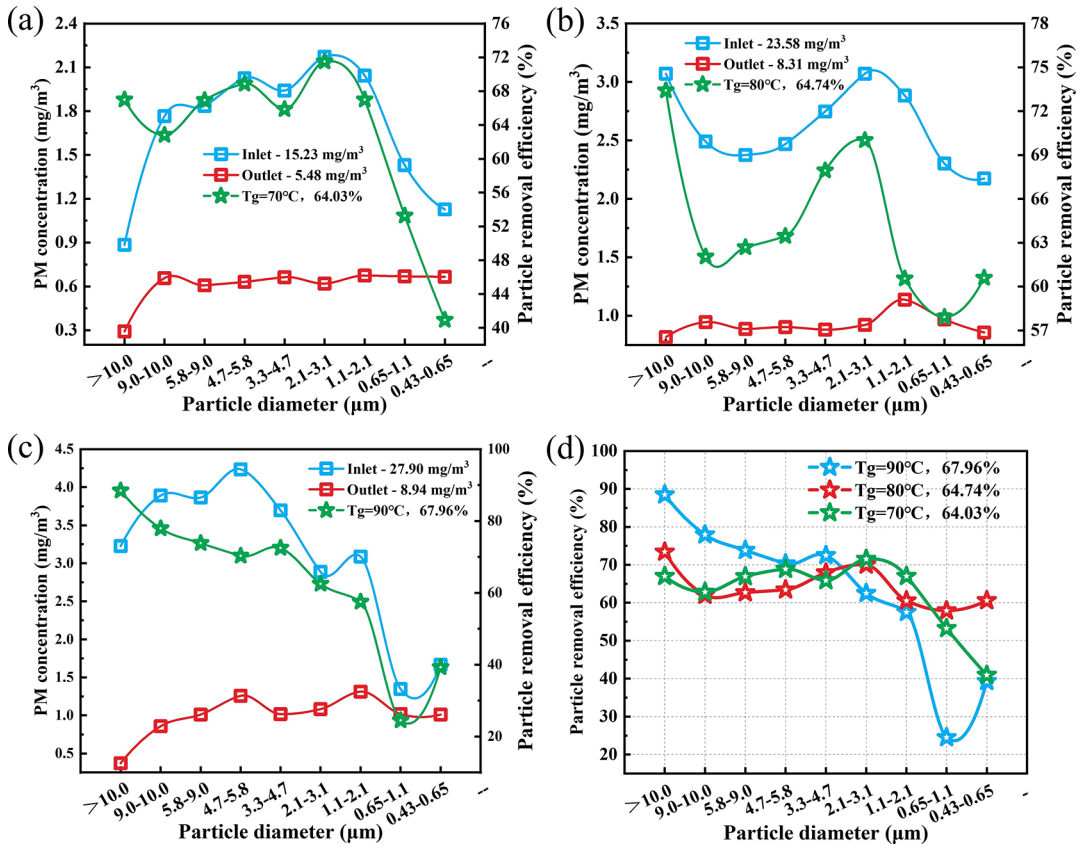

Figure 5. Effect of the flue gas temperature on the particle removal performance ((a): T_g = 70 °C; (b): T_g = 80 °C; (c): T_g = 90 °C; and (d): comparison of removal performance at different temperature).

constant at 65 m^3/h. According to Figure 5, the flue gas temperature had no significant effect on the scrubbing effect of the SCSB-PRD. When the flue gas temperatures were 70, 80, and 90 °C, the scrubbing effects were 64.03, 64.74, and 67.96%, respectively. The outlet PM concentration was less than 10 mg/m^3. When the flue gas temperature increased from 70 to 90 °C, the particle removal efficiency increased slightly. The results indicated that under the premise of a small temperature difference, the effect of particle thermophoresis on the scrubbing process of the SCSB-PRD was limited, which was similar to the results of a previous study.[48]

For large particle scrubbing ($PM_{2.5-10}$), the removal efficiency reached more than 60%. The overall removal efficiency decreased with a decrease in the particle size, and the removal efficiency of submicrometer particles was unsatisfactory. Submicron particles belong to the penetrating particle size range, and particles larger than 1 μm are strongly affected by the inertial force[26] and can move to the surface of the bubble liquid film and be captured by the liquid film.[35]

3.3. Effect of the Scrubbing Liquid Volume on the Particle Removal Performance. The bubbling space of the SCSB-PRD device was W150H37. In the experiment, the scrubbing volume was adjusted by adjusting the liquid level height to explore the influence of different liquid volumes and bubbling states on the particle removal performance. The liquid level height, H, increased from 30 to 60 mm, and the flue gas flow was 65 m^3/h. As shown in Figure 6, with an increase in the liquid–gas ratio, the overall particle removal efficiency first increased and then decreased, and the particle size with higher particle removal efficiency was >9 μm. As the particle size decreased, the removal efficiency gradually decreased due to the particle motion mechanism.

As shown in Figure 7, the gas–liquid bubbling flow state could be divided into three types: the bubbling state, the foam bubbling state, and the jet-bubbling state.[49] The bubbling state had a large bubble size and a large number of bubbles. The bubbling state occurs only at a low flue gas velocity and is relatively rare in the industry. The foam bubbling state and jet-bubbling state were the primary gas–liquid flow states in the SCSB-PRD. The primary feature of the foam bubbling state is that a large number of bubbles are generated in the scrubbing area and the primary removal mechanism of pollutants is bubble internal-surface scrubbing. In contrast, the primary feature of the jet-bubbling state is that a large number of large and small bubbles are generated in the scrubbing area and the liquid is agitated by the flue gas with a large flow rate. This process partially generates fine droplets and purifies the flue gas under the synergistic action of the bubbles and droplets.

When H = 30 mm, due to the low liquid–gas ratio, sparse bubbles formed, the gas–liquid contact was unsatisfied, and there was also an insufficient gas–liquid contact time. This resulted in an overall poor particle removal efficiency, and the removal efficiency of the full-size particles was less than 50%. When H = 40 mm, the gas–liquid contact was more sufficient and more bubbles and droplets formed. This enhanced the removal ability of the full-size particles. When H = 60 mm, the excessive ratio of liquid to gas caused inordinate resistance of the scrubber, and the gas–liquid contact state changed from the jet-bubbling to the foam bubbling state with a smaller

https://doi.org/10.1021/acsomega.3c08250
ACS Omega 2024, 9, 9321−9330

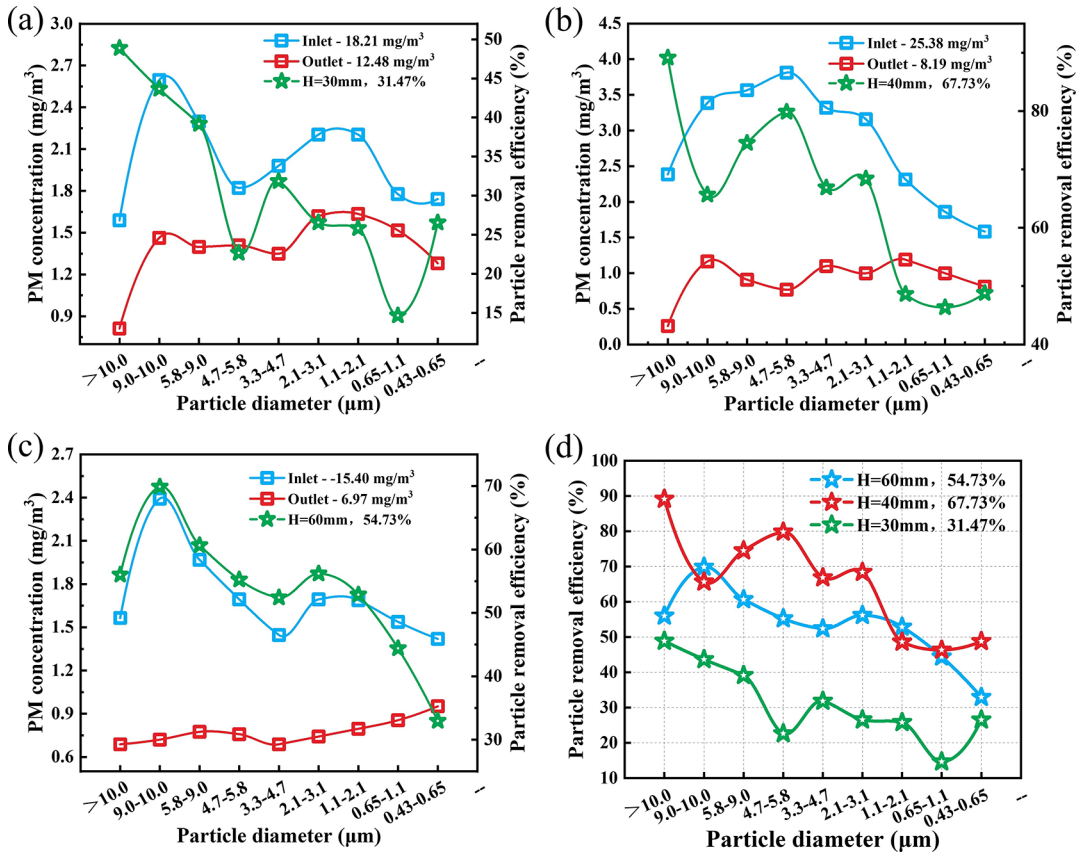

Figure 6. Effect of the scrubbing liquid volume on the particle removal performance ((a): H = 30 mm; (b): H = 40 mm; (c): H = 60 mm; and (d): comparison of removal performance with different scrubbing liquid volume).

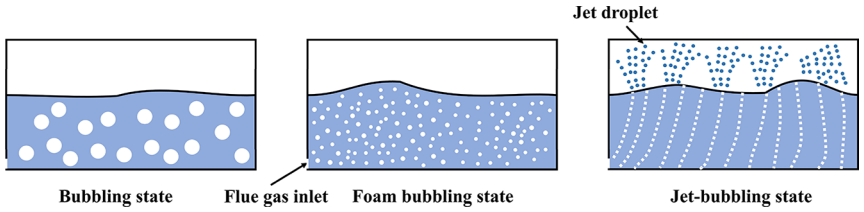

Figure 7. Gas−liquid bubbling contact state.

interface contact area. Refer to the Supporting Information for foam and jet-bubbling videos.

3.4. Effect of the Scrubbing Space on the Particle Removal Performance. To explore the installation spacing between the bubbling devices in the actual industrial application of flue gas purification, the height of the liquid level was maintained at 40 mm and the width of the bubbling space of the SCSB-PRD device was maintained at W150 by changing the length of the scrubbing space. The effect of different bubbling states on the particle removal performance was then explored. During the experiment, the flue gas temperature was maintained at 90 °C, and the flue gas flow rate was 65 m^3/h.

The results are depicted in Figure 8. When the bubbling area was W150L37, a jet-bubbling gas−liquid contact area was formed in the longitudinal space. When the scrubbing liquid increased, the flue gas velocity in the gas−liquid contact area decreased and the high gas−liquid contact state changed from jet-bubbling to foam bubbling with a smaller interface contact area that reduced the particle capture efficiency. The removal efficiency reached a gap of greater than 30%. As the scrubbing space increased to L = 67 mm due to an increase in the liquid−gas ratio and increased gas−liquid contact possibility, although the gas−liquid contact state changed to the foam bubbling state with a smaller gas−liquid contact area, the removal efficiency increased with an increased liquid−gas ratio. As the scrubbing space continued to increase to L = 77 mm, due to the great scrubbing resistance, the gas−liquid contact state was partially transferred from the foam bubbling state to the bubbling state, resulting in a decrease in its particle removal performance. Additionally, Figure 8 shows that the jet-bubbling state had a higher fine particle ($PM_{<10}$) removal performance than the foam bubbling state.

3.5. Effect of the Flue Gas Flow Rate on the Particle Removal Performance. To explore the effect of the flue gas flow rate on the particle removal performance during the actual application of the SCSB-PRD device, the scrubbing space was maintained at L57W150H40, changing the flue gas flow velocity to change the flow rate, and the gas−liquid scrubbing state was in the foam bubbling state in the L57W150H40 SCSB-PRD. During the experiment, the flue gas temperature was maintained at 90 °C.

https://doi.org/10.1021/acsomega.3c08250
ACS Omega 2024, 9, 9321−9330

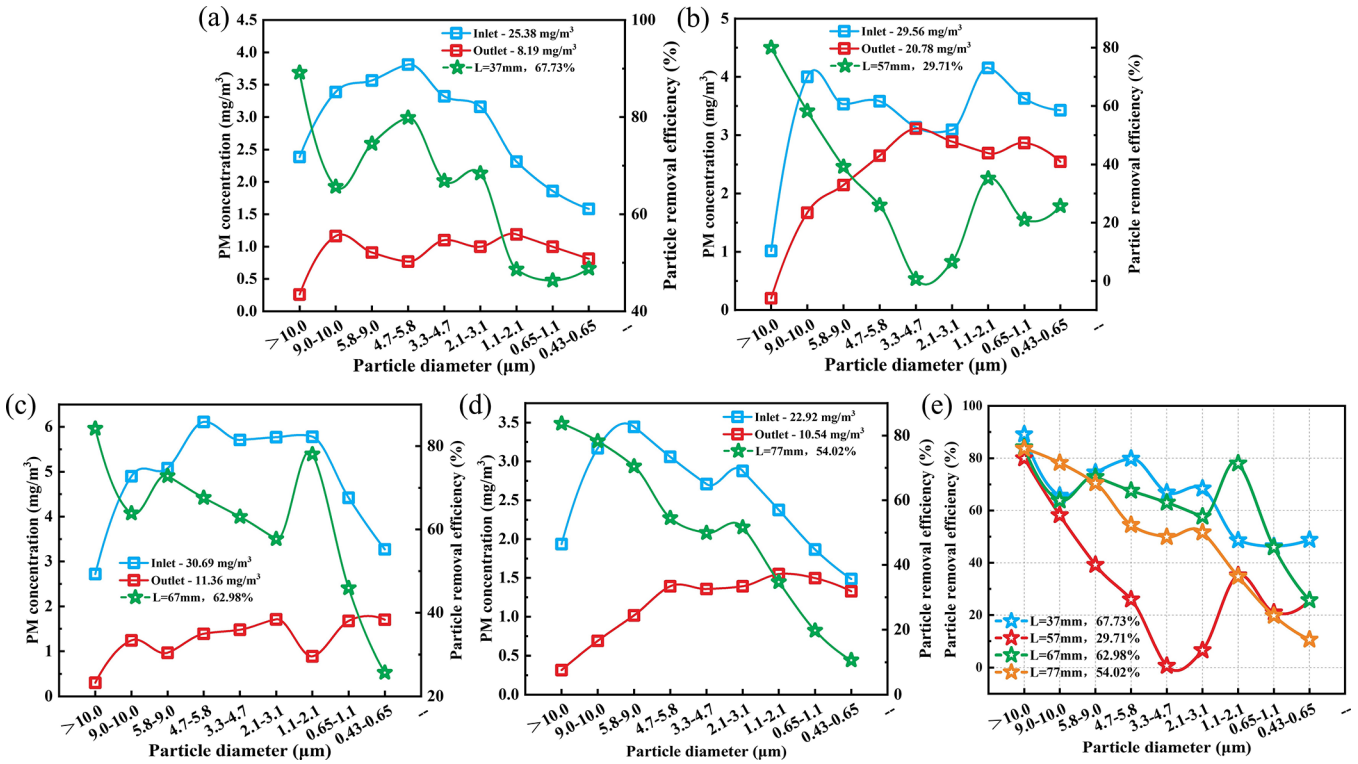

Figure 8. Effect of the scrubbing space on the particle removal performance ((a): L = 37 mm; (b): L = 57 mm; (c): L = 67 mm; (d): L = 77 mm; and (e): comparison of removal performance with different scrubbing space.

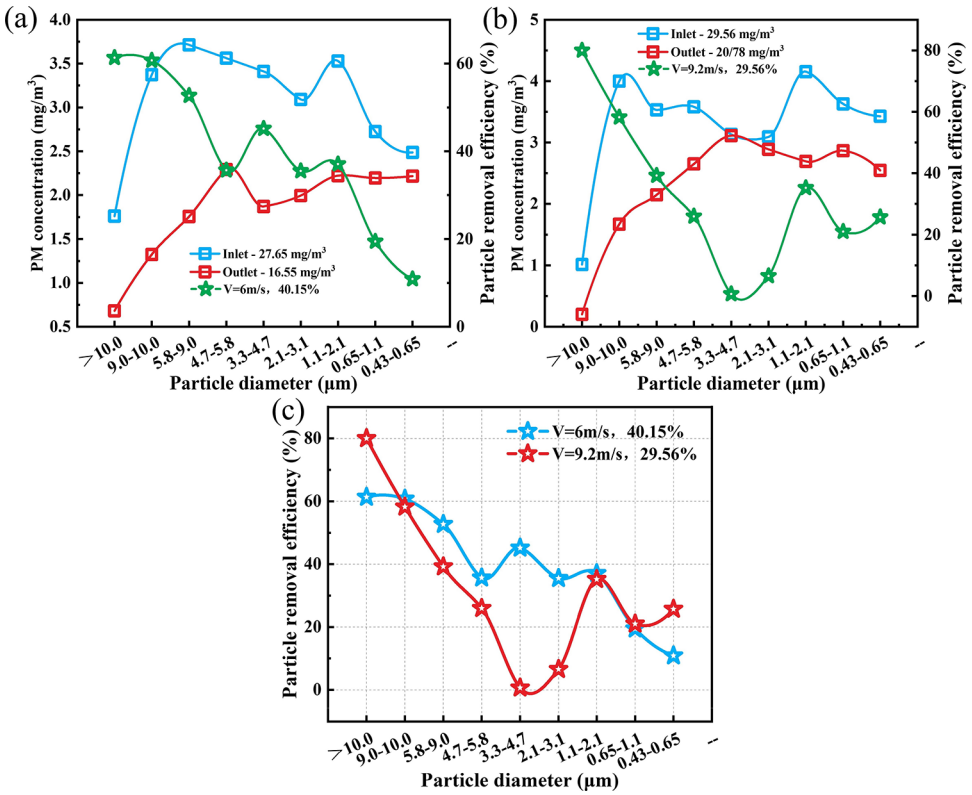

Figure 9. Effect of the flue gas flow rate on the particle removal performance ((a): V = 6 m/s; (b): V = 9.2 m/s; and (c): comparison of removal performance with different flue gas flow rate).

As shown in Figure 9, when the flue gas flow rates were 6 and 9.2 m/s, the flue gas flow rates were 42 and 65 m^3/h, respectively, when the gas−liquid state was in the foam bubbling state. When the liquid−gas ratio increased, the flue gas flow velocity decreased in the scrubbing area, and the gas−liquid contact time increased, thereby improving the particle

https://doi.org/10.1021/acsomega.3c08250
ACS Omega 2024, 9, 9321−9330

capture efficiency. Thus, under the same gas−liquid flow state, an increase in the liquid−gas ratio was conducive to PM purification.

3.6. Particle Removal Mechanism. The particle removal mechanism is shown in Figure 10. The flue gas entrained with

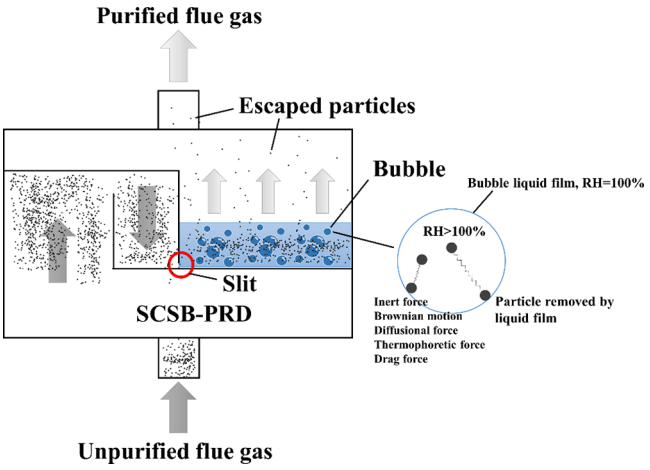

Figure 10. Schematic of SCSB-PRD and particle removal mechanism.

particles entered the particle scrubbing device through a 20 mm high slit, aroused a large number of bubbles, and removed particles by contacting the bubble internal liquid film due to the particle motion mechanism that included the inert force, Brownian motion, the diffusional force, the thermophoretic force, and the drag force.[35,50]

4. CONCLUSIONS

In this work, to achieve the coal-fired flue gas PM ultraultra-low emission goal, an SCSB-PRD based on the bubbling characteristics of the wet scrubbing device was designed and its particle removal performance was tested. Furthermore, the influences of different scrubbing parameters (e.g., flue gas temperature, scrubbing liquid volume, scrubbing space, and flue gas flow rate) were explored, and the following conclusions were obtained:

1. After installation of the SCSB-PRD device, the particle removal efficiency reached greater than 60%, and the target PM concentration at the outlet of the WFGD device was less than 10 mg/m^3. Hence, this work provides a feasible transformation path for ultraultra-low emissions of PM from coal-fired power plants.
2. When the temperature difference was not significant, the flue gas temperature had no obvious effect on the SCSB-PRD scrubbing effect. Therefore, the weak effect of thermophoresis occurred for the enhanced capture of PM under the conditions of a small temperature difference.
3. Compared with the foam bubbling gas−liquid contact state, the jet-bubbling gas−liquid contact state was more conducive to the removal of PM. The liquid−gas ratio and the scrubber layout had significant influences on the particle removal performance.
4. In comparison to the foam bubbling state, the removal efficiency of fine particles in the jet-bubbling state was improved by more than 30%. This was because the particle removal method in the spray state consisted of cooperative removal of the bubble liquid film coupled with fine droplets.

ASSOCIATED CONTENT

Supporting Information

The Supporting Information is available free of charge at https://pubs.acs.org/doi/10.1021/acsomega.3c08250.

Detailed structure and installed position of the bubble cap tray scrubbing layer, schematic of the Andersen cascade impactor sampling device, Andersen cascade impactor simulates the human respiratory system, and plot showing the repeated experiments with similar particles concentrations in the SCSB-PRD (PDF)
Gas liquid foam bubbling state in SCSB-PRD (MP4)
Gas liquid jet-bubbling state in SCSB-PRD (MP4)

AUTHOR INFORMATION

Corresponding Authors

Renjie Zou − *State Key Laboratory of Coal Combustion (SKLCC), School of Energy and Power Engineering, Huazhong University of Science and Technology, Wuhan, Hubei 430074, China;* orcid.org/0000-0003-3146-4716; Email: rjzou@hust.edu.cn

Guangqian Luo − *State Key Laboratory of Coal Combustion (SKLCC), School of Energy and Power Engineering, Huazhong University of Science and Technology, Wuhan, Hubei 430074, China; Shenzhen Huazhong University of Science and Technology Research Institute, Shenzhen, Guangdong 518052, China*; Email: guangqian.luo@mail.hust.edu.cn

Authors

Can Fang − *State Key Laboratory of Coal Combustion (SKLCC), School of Energy and Power Engineering, Huazhong University of Science and Technology, Wuhan, Hubei 430074, China*

Yi Xiao − *State Key Laboratory of Coal Combustion (SKLCC), School of Energy and Power Engineering, Huazhong University of Science and Technology, Wuhan, Hubei 430074, China*

Wencong Qiu − *State Key Laboratory of Coal Combustion (SKLCC), School of Energy and Power Engineering, Huazhong University of Science and Technology, Wuhan, Hubei 430074, China*

Haoyu Zhang − *State Key Laboratory of Coal Combustion (SKLCC), School of Energy and Power Engineering, Huazhong University of Science and Technology, Wuhan, Hubei 430074, China*

Tianyu Zhao − *State Key Laboratory of Coal Combustion (SKLCC), School of Energy and Power Engineering, Huazhong University of Science and Technology, Wuhan, Hubei 430074, China*

Hong Yao − *State Key Laboratory of Coal Combustion (SKLCC), School of Energy and Power Engineering, Huazhong University of Science and Technology, Wuhan, Hubei 430074, China*

Complete contact information is available at: https://pubs.acs.org/10.1021/acsomega.3c08250

Author Contributions

C.F. (first author): conceptualization, methodology, data curation, and writing - original draft; Y.X.: data curation, writing - original draft; W.Q.: data presentation, instrumentation; H.Z.: resources, writing - review & editing; T.Z.: visualization, experiment; R.Z. (corresponding author): visual-

https://doi.org/10.1021/acsomega.3c08250
ACS Omega 2024, 9, 9321−9330

ization, writing - review & editing, funding acquisition; G.L.: supervision, funding acquisition; H.Y.: supervision, project administration, and funding acquisition.

Notes

The authors declare no competing financial interest.

We are sure that the manuscript has not been published elsewhere and that it has not been submitted simultaneously for publication elsewhere. The authors declare no competing financial interests.

Our study does not involve human subjects. Written informed consent for publication of this paper was obtained from the Huazhong University of Science and Technology, Shenzhen Huazhong University of Science and Technology Research Institute and all authors.

■ ACKNOWLEDGMENTS

The authors gratefully acknowledge the financial support provided by the National Key Research and Development Program of China (No. 2022YFB4100202), the National Natural Science Foundation of China (Nos. 52076093 and 52206142), the Shenzhen Science and Technology Program (JSGG20201102153400001), and the Postdoctoral Creative Research Funding of Hubei Province.

■ REFERENCES

(1) Pudasainee, D.; Kurian, V.; Gupta, R. 2 - Coal: Past, Present, and Future Sustainable Use. In: Letcher, T.M., Ed.; *Future Energy*, third ed.; Elsevier: 2020; pp 21−48.

(2) International Energy Agency. *World Energy Outlook 2021*; Paris, 2021.

(3) International Energy Agency. *Coal 2021*; Paris, 2021.

(4) The Central People's Government of the People's Republic of China. The 14th Five-Year Plan for National Economic and Social Development of the People's Republic of China and the Outline of Vision Goals for 2035, 2021.

(5) State Council of the People's Republic of China. Action Plan to Peak Carbon by 2030, 2021.

(6) State-owned Assets Supervision and Administration Commission of State Council (SASAC). Guiding Opinions on Promoting the High-Quality Development of Central Enterprises and Doing a Good Job in Carbon Peak and Carbon Neutralization, 2021.

(7) Shan, B.; Xingpei, J.; Yao, L.; Ma, J.; Wu, C.; Duan, J. Evolving Tendency of Electric Supply and Demand Pattern under the Circumstances of High-Quality Energy Development. *Electric Power* **2021**, *54* (1−9), 18.

(8) Gasparotto, J.; Martinello, D. B. Coal as an energy source and its impacts on human health. *Energy Geosci.* **2021**, *2*, 113−120.

(9) Hendryx, M.; Zullig, K. J.; Luo, J. Impacts of Coal Use on Health. *Annu. Rev. Public Health* **2020**, *41*, 397−415.

(10) Finkelman, R. B.; Tian, L. The health impacts of coal use in China. *Int. Geol. Rev.* **2018**, *60*, 579−589.

(11) Institute for Health Metrics and Evaluation (IHME). *GBD Compare Data Visualization*; IHME, University of Washington: Seattle, WA, 2020.

(12) State Council of the People's Republic of China. Action Plan of Air Pollution Prevention and Control, **2013**.

(13) State Council of the People's Republic of China. Action plan 2014 −2020 for transforming the coal fired power industry and upgrading energy conservation and emission reduction, 2014.

(14) State Council of the People's Republic of China. Three-year action plan for cleaner air, 2018.

(15) Ministry of Environmental Protection, National Development and Reform Commission, National Energy Administration. Full implementation of the ultra-low emission and energy-saving transformation work plan for coal-fired power plants, 2015.

(16) Ministry of Ecological Environment of the People's Republic of China. Bulletin of Ecology and Environment Status of China, (2013−2020).

(17) W.H. Organization. *Air quality guidelines: particulate matter (PM2.5 and PM10), ozone, nitrogen dioxide, sulfur dioxide and carbon monoxide*; World Health Organization: 2021.

(18) Zhang, X. *Emission standards and control of PM2. 5 from coal-fired power plants*; IEA Clean Coal Centre: London, 2016.

(19) International Energy Agency. *Technology Roadmap - High-Efficiency, Low-Emissions Coal-Fired Power Generation*; Paris, 2012.

(20) Department of Ecology and Environment of Jiangsu Province. Emission standard of air pollutants for coal-fired power plants, 2021.

(21) Du, Z.; Jiang, J.; Zhang, Y.; Wei, H.; Zhu, Y. Analysis of Particle Removal Characteristics on Wet Electrostatic Precipitator for Ultra-low Emission Coal-fired Power Unit, Chinese. *J. Electr. Eng.* **2020**, *40*, 7675−7683.

(22) Department of Ecology and Environment of Jiangsu Province. The explanation for the compilation of "Emission Standard of Air Pollutants for Thermal Power Plants", 2020.

(23) Fang, C.; Zou, R.; Luo, G.; Ji, Q.; Sun, R.; Hu, H.; Li, X.; Yao, H. CFD simulation design and optimization of a novel zigzag wave-plate mist eliminator with perforated plate. *Applied Thermal Engineering* **2021**, *184*, No. 116212.

(24) Zou, R.; Luo, G.; Fang, C.; Zhang, H.; Li, Z.; Hu, H.; Li, X.; Yao, H. Modeling Study of Selenium Migration Behavior in Wet Flue Gas Desulfurization Spray Towers. *Environ. Sci. Technol.* **2020**, *54*, 16128−16137.

(25) Ardon-Dryer, K.; Huang, Y. W.; Cziczo, D. J. Laboratory studies of collection efficiency of sub-micrometer aerosol particles by cloud droplets on a single-droplet basis. *Atmos. Chem. Phys.* **2015**, *15*, 9159−9171.

(26) Wang, A.; Song, Q.; Yao, Q. Study on inertial capture of particles by a droplet in a wide Reynolds number range. *J. Aerosol Sci.* **2016**, *93*, 1−15.

(27) Wu, Q.; Gu, M.; Du, Y.; Zeng, H. Synergistic removal of dust using the wet flue gas desulfurization systems. *R. Soc. Open Sci.* **2019**, *6*, No. 181696.

(28) Rafidi, N.; Brogaard, F.; Chen, L.; Håkansson, R.; Tabikh, A. CFD and experimental studies on capture of fine particles by liquid droplets in open spray towers, Sustainable. *Environ. Res.* **2018**, *28*, 382−388.

(29) Huang, Y.; Zheng, C.; Li, Q.; Zhang, J.; Guo, Y.; Zhang, Y.; Gao, X. Numerical simulation of the simultaneous removal of particulate matter in a wet flue gas desulfurization system. *Environ. Sci. Pollut. Res.* **2020**, *27*, 1598−1607.

(30) Liang, Y.; Li, Q.; Ding, X.; Wu, D.; Wang, F.; Otsuki, T.; Cheng, Y.; Shen, T.; Li, S.; Chen, J. Forward ultra-low emission for power plants via wet electrostatic precipitators and newly developed demisters: Filterable and condensable particulate matters. *Atmos. Environ.* **2020**, *225*, No. 117372, DOI: 10.1016/j.atmosenv.2020.117372.

(31) Jiang, B.; Xie, Y.; Xia, D.; Liu, X. A potential source for PM2.5: Analysis of fine particle generation mechanism in Wet Flue Gas Desulfurization System by modeling drying and breakage of slurry droplet. *Environ. Pollut.* **2019**, *246*, 249−256.

(32) Pan, D.; Gu, C.; Zhang, D.; Shi, H. Investigation on the relationship between slurry droplet entrainment and fine particle emission in the limestone-gypsum WFGD system. *Energy Sources Part A* **2020**, *42*, 1691−1704.

(33) Shen, J. *Numerical Study on Moisture Reduction Mechanism of WFGD System*; Southeast University: 2019.

(34) Wang, Q.; Chen, X.; Gong, X. The Particle Removing Characteristics in a Fixed Valve Tray Column. *Ind. Eng. Chem. Res.* **2013**, *52*, 3441−3452.

(35) Pan, W.; Chen, X.; Dai, G.; Wang, F. Enhanced Effect of Bubble Deformation on Internal Particle Transport. *Ind. Eng. Chem. Res.* **2020**, *59*, 905−918.

(36) Chen, Z.; Jiang, Z.; Wang, H.; You, C. *Experimental Investigation on the Synergetic Removal of SO_3, SO_2, and Particulate*

https://doi.org/10.1021/acsomega.3c08250
ACS Omega 2024, 9, 9321−9330

Matter in a Gas−Liquid Flow Pattern-Controlling Column Coupled with Ultrasonic Wave; Industrial & Engineering Chemistry Research: 2020.
(37) Wei, T.; Li, X.; Wang, D. Identification of gas-liquid two-phase flow patterns in dust scrubber based on wavelet energy entropy and recurrence analysis characteristics. *Chem. Eng. Sci.* **2020**, *217*, No. 115504, DOI: 10.1016/j.ces.2020.115504.
(38) Bandyopadhyay, A.; Biswas, M. N. Fly-Ash Scrubbing in a Tapered Bubble Column Scrubber. *Process Safety and Environmental Protection* **2006**, *84*, 54−62.
(39) Wang, Q.; Chen, X.; Guo, Z.; Gong, X. An experiment investigation of particle collection efficiency in a fixed valve tray washing column. *Powder Technol.* **2014**, *256*, 52−60.
(40) Shenastaghi, F. K.; Roshdi, S.; Kasiri, N.; Hasan Khanof, M. CFD simulation and experimental validation of bubble cap tray hydrodynamics. *Sep. Purif. Technol.* **2018**, *192*, 110−122.
(41) Blinichev, V.; Postnikova, I.; Szatko, W.; Krawczyk, J. Influence of the Main Factors on the Efficiency of Wet Vortex Dust Collectors. *Izv. Vyssh. Uchebn. Zaved., Khim. Khim. Tekhnol.* **2019**, *62*, 98−105, DOI: 10.6060/IVKKT.20196206.5927.
(42) Chen, Z.; Jiang, Z.; You, C.; Wang, H. Experimental investigation on flue gas purification and gas-liquid multiphase flow in a spraying column with perforated plate, The. *Can. J. Chem. Eng.* **2020**, *98*, 1059−1068.
(43) Terasaka, K.; Sasada, Y.; Kobayashi, D.; Fujioka, S. Submilli-Bubble Dispersion from a Slit Orifice into Water. *J. Chem. Eng. Jpn.* **2011**, *44*, 140−145.
(44) Mirzaee, I.; Charmchi, M.; Sun, H.; Song, M. Micro Scale Air Sampling Devices: A Numerical Study. In *ASME 2016 International Mechanical Engineering Congress and Exposition*; 2016.
(45) Mirzaee, I.; Song, M.; Charmchi, M.; Sun, H. A microfluidics-based on-chip impinger for airborne particle collection. *Lab Chip* **2016**, *16*, 2254−2264.
(46) Andersen, A. A. New sampler for the collection, sizing, and enumeration of viable airborne particles. *J. Bacteriol.* **1958**, *76*, 471−484.
(47) Nahar, K.; Gupta, N.; Gauvin, R.; Absar, S.; Patel, B.; Gupta, V.; Khademhosseini, A.; Ahsan, F. In vitro, in vivo and ex vivo models for studying particle deposition and drug absorption of inhaled pharmaceuticals. *Eur. J. Pharm. Sci.* **2013**, *49*, 805−818.
(48) Li, C.; Ji, B.; Song, Q.; Yao, Q. Numerical Simulation of Synergetic Removal of Particulate Matter by Spraying During Wet Flue Gas Desulfurization. *Proc. CSEE* **2019**, *39*, 1070−1078.
(49) Levenspiel, O. *Chemical reaction engineering*; John Wiley & Sons: 1998.
(50) Wang, Q.; Chen, X.; Gong, X. Theoretical and experimental investigation on the characteristics of fly-ash scrubbing in a fixed valve tray column. *AlChE J.* **2013**, *59*, 2168−2178.

https://doi.org/10.1021/acsomega.3c08250
ACS Omega 2024, 9, 9321−9330